RESEARCH ARTICLE

A soft tissue fabricated using a freeze-drying technique with carboxymethyl chitosan and nanoparticles for promoting effects on wound healing

Atiyeh Raisi[1], Azadeh Asefnejad[1], Maryam Shahali[2], Zahra Doozandeh[3], Bahareh Kamyab Moghadas[4], Saeed Saber-Samandari[5], Amirsalar Khandan[5,*]

[1] Department of Biomedical Engineering, Science and Research Branch, Islamic Azad University, Tehran, Iran

[2] Department of Quality Control, Research and Production Complex, Pasteur Institute of Iran, Tehran, Iran

[3] Master of Nursing Science, Islamic Azad University, Isfahan (Khorasgan) Branch, Esfahan, Iran

[4] Department of Chemical Engineering, Shiraz Branch, Islamic Azad University, Shiraz, Iran

[5] New Technologies Research Center, Amirkabir University of Technology, Tehran, Iran

ARTICLE INFO

Article History:
Received 2019-12-09
Accepted 2020-04-17
Published 2020-10-01

Keywords:
Wound dress
Carboxymethyl Chitosan
Soft Tissue
Freeze Drying
Tissue Engineering

ABSTRACT

Objective(s): Many people suffer from skin injuries due to various problems such as burns and accidents. Therefore, it is essential to shorten treatment time and providing strategies that can control the progression of the wound that would be effective in wound healing process and also reduce its economic costs.

Methods: The present study aimed to prepare a nanocomposite dressing (NCD) composed of carboxymethyl chitosan (CMC), and Fe_2O_3 nanoparticles by a method called freeze-drying (FD) technique. The effect of different weight percentages of Fe_2O_3 (0, 2.5, 5, and 7.5 wt%) reinforcement on mechanical and biological properties such as tensile strength, biodegradability, and cell behavior was evaluated. Also, the X-ray diffraction (XRD) and scanning electron microscopy (SEM) analysis were used to characterize the soft porous membrane. The biological response in the physiological saline was performed to determine the rate of degradation of NCD in phosphate buffer saline (PBS) for a specific time.

Results: The obtained results demonstrated that the wound dress was porous architecture with micron-size interconnections. In fact, according to the results, as the magnetite nanoparticles amount increases, the porosity increases too. On the other hand, the tensile strength was 0.32 and 0.85 MPa for the pure sample and the sample containing the highest percentage of magnetic nanoparticles, respectively. Besides, the cytotoxicity of this nanocomposite was determined by MTT assays for 7 days and showed no cytotoxicity toward the growth of fibroblasts cells and had proper in vitro biocompatibility. The obtained results revealed that NCD had remarkable biodegradability, biocompatibility, and mechanical properties. Therefore, NCD composed of CMC and Fe_2O_3 nanoparticles was introduced as a promising candidate for wound healing applications.

Conclusions: According to the obtained results, the optimum NCD specimen with 5 wt% Fe_2O_3 has the best mechanical and biological properties.

How to cite this article
*Raisi A., Asefnejad A., Shahali M., Doozandeh Z., Kamyab Moghadas B., Saber-Samandari S., Khandan A.S. A soft tissue fabricated using a freeze-drying technique with carboxymethyl chitosan and nanoparticles for promoting effects on wound healing. J. Nanoanalysis., 2020; 7(4): -12. DOI: 10.22034/jna.***.*

INTRODUCTION

Traditional wounds such as gauzes and bandages, create a dry environment on the wound by absorbing excessive secretions [1-4]. Several researchers reject the popular belief that the effect of dry wound dressing is to accelerate the healing process when used with a moisture-retaining dressing, is much faster than when the wounds are exposed only to dry air [5-8]. Other important features of wound dressings are that they have porosity, adhesion, and good mechanical strength,

* Corresponding Author Email: *amir_salar_khandan@yahoo.com*

low price, easy to use, and also the ability to swap without damaging the wound [9-11]. It should be noted that all of the characteristics listed in a single dressing are not applied to all wounds, and each injury must be carefully evaluated individually, and then the appropriate dressing selected [12-17]. Nowadays, there are several different dressings like hydrogels [16], foams [17], films [18-19], membranes [18] and other available antibacterial creams as an agent to use in combination with polymers for wounds healing. Recently, the use of natural polymers due to their high biocompatibility, biodegradability, and similarity to body tissues have been considered in the treatment of wounds [20-24]. Therefore, the researchers have been focused on polymers such as hyaluronic acid [25], collagen [26], alginate [1, 12, 27], elastin [29], chitosan [30], gelatin [31-35], nanofibrous polycaprolactone [36, 69] due to their excellent biodegradability, non-toxicity, and ability to carry several therapeutic agents like growth factors (GFs) [32]. On the other hand, polymers have poor mechanical properties, and composite preparation is one of the ways to improve their mechanical properties. Polymeric-ceramic composites have particular importance [36-39]. Studies have shown that by using bioceramics, along with polymeric materials, in addition to achieving better mechanical properties such as elastic modulus, the degree of biocompatibility will also increase dramatically [33-40]. One of the bioceramics of interest in tissue engineering is the bioceramics of diopside contains silicon and magnesium to an appropriate extent [41-48]. Diopside, with the chemical composition of $CaMgSi_2O_6$, magnesium-based silicate ceramics with higher mechanical stability and lower degradation rates than bioglass and other active ceramics [47-48] and its application to soft tissue engineering, looks good in particular when slow destruction rates are desirable [43-45]. Also, in the present study, magnetic nanoparticles were used to enhance antibacterial activity to achieve the best and most ideal mechanical and biological properties in addition to bioceramic diopside. The use of magnetic nanoparticles has had a long history in medicine, as Hippocrates, used magnetic iron oxide and hematite to stop and control the bleeding [49-51]. Also, in the first century, researchers invent magnetite powders based on their unique physical, chemical, thermal and mechanical properties. Magnetic nanoparticles have shown great potential for various medical applications. Among the available nanomaterials, hematite has a chemical structure of Fe_2O_3 and has the least toxicity due to the presence of iron and zinc in its composition and the human body's need for these elements [49-51]. One of the reasons for using these nanoparticles is their antibacterial properties and disinfectant in wound conditions. Various techniques are used for the preparation of the membrane and scaffold, such as 3D printing [52-54], electrospinning [7, 27], and freeze-drying technique [11-12]. Preparation of composite using the various methods as medical or industrial applications needs to be investigated for their mechanical performance. However, several simulation software can predict their mechanical properties without laboratory tests such as molecular dynamics, classical solution methods, finite element analysis and micromechanical model [55-68]. The application of this software causes the researchers to used and model different materials with different properties as synergic material in the software without an experimental analysis which is time-consuming and expensive [69-75]. In the current study, we aim to realize a novel nanocomposite material with excellent biocompatibility and then prepared a flexible and microporous nanocomposite wound dress by the freeze-drying process. In the present study, the morphology, antibacterial activity, physical and chemical properties, and biocompatibility were evaluated, providing the basis for alternative materials for wound healing.

MATERIALS AND METHODS

Materials Preparation

For the preparation of nanocomposite dressing (NCD), carboxymethyl-chitosan (CMC) powder with the chemical formula of $C_{20}H_{37}N_3O_{14}$ was purchased from Sigma–Aldrich, The USA for matrix as can be seen in Fig. 1. The CMC solvent was selected water with the addition of 1% vol. CH_3COOH in the 180 ml of deionized water [$C_6H_8O_7H_2O$, Mw = 192.124, Sigma–Aldrich, USA], Diopside (Dp) powder ($CaMgSi_2O_6$, 50-100 nm, 90% purity) synthesized according to the previous work and magnetic nanoparticles (Zn-contain α-Fe_2O_3, 20-40 nm, 90% purity) was purchased from Merck [41-42]. This work aims to produce a novel Zn-Fe_2O_3-containing wound dress based on CMC.

Methods Procedure

The NCD made of CMC/Dp/Fe_2O_3 was

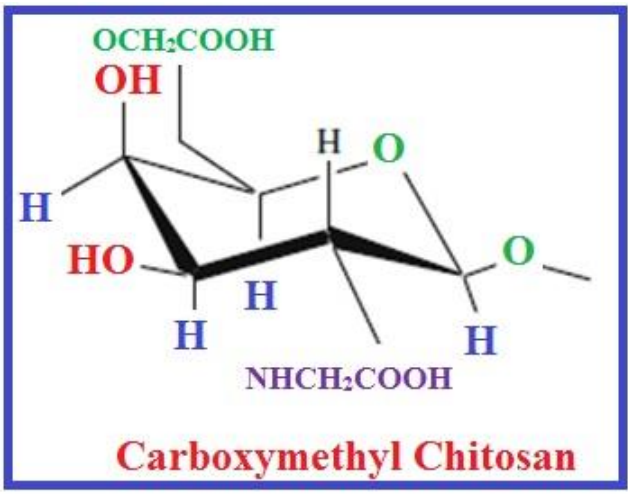

Fig.1. Chemical Structure of CarboxyMethyl Chitosan (CMC) biopolymer

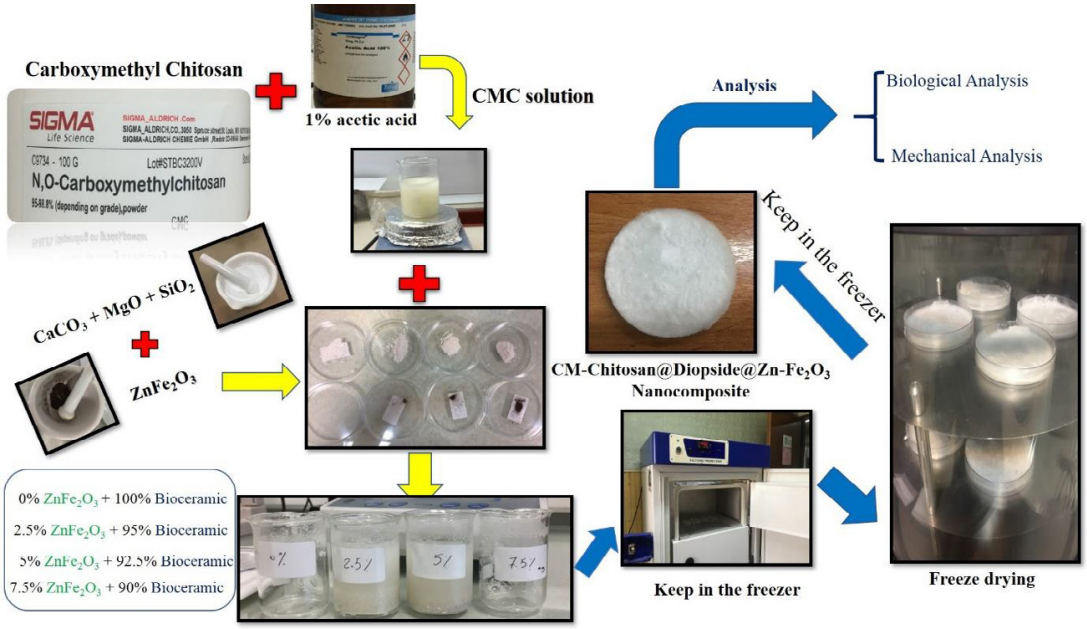

Fig. 2. Schematic illustration of the fabrication NCD using FD technique.

prepared by following the materials selection and materials preparation procedures, as can be seen in Fig. 2. Briefly, solutions were prepared by dissolving 3 g CMC powder in 180 ml deionized water and 1% vol acetic acid solution and then continuously stirred for 4 hours at 600 rpm at 50°C to form a homogeneous suspension of a natural polymer, the following process was carried out until a homogeneous solution was obtained. The bioceramic powder (Dp) and different weight fraction of Fe_2O_3 (0, 2.5, 5, and 7.5 wt%) were mixed and milled for 30 min in the mechanical mixer (IKA, Germany). The samples were prepared in accordance with Table 1. The final mixtures were stirred at 50°C for 4 hours to provide homogenous dispersion of the Dp-Fe_2O_3 solution. After that, 0.25% glutaraldehyde ($C_5H_8O_2$) was added to resultant polymeric solutions as a cross-linker. A certain amount of resultant solution was transferred to Petri dishes according to the percentage of specific weights and froze at -65°C for 24 hours. After the emulsion was removed from the freezer,

Table 1. Weight percentages of NCD bio-nanocomposite wound dress

SAMPLE	sample	Dp (W%)	MNPs (W%)
CMC-Dp	CMC- Dp -0 wt% Zn+Fe_2O_3	0.5	0
CMC-DpZn	CMC- Dp -2.5 wt% Zn+Fe_2O_3	0.5	2.5
CMC-DpZn$_1$	CMC- Dp -5 wt% Zn+Fe_2O_3	0.5	5
CMC-DpZn$_2$	CMC- Dp -7.5 wt% Zn+Fe_2O_3	0.5	7.5

the frozen samples were placed in a freeze-drying (FD) machine (DorsaTech company, Tehran, Iran) at -45°C for 48 hours to eliminate the moisture and water. However, the scaffolds were removed from the FD machine and then prepared for different testing and analysis. The obtained NCD specimen with increasing α-Fe_2O_3 amount was referred to as CDp, CDpZn, CDpZn1, and CDpZn2, respectively. A summary of the combination of bioceramics and polymers is Tabulated in Table 1.

MATERIALS CHARACTERIZATION

Mechanical Testing of the NCD

Mechanical behavior of NCD, including tensile strength and elastic modulus using tensile machine according to ASTM-20 standard (SANTAM-STM50) at speed rate (0.5 mm/min), was conducted at New Technology Research Center, The Amirkabir University of Technology. The specimens used in this experiment consisted of four porous samples with a porosity of 100 microns in diameter with 8 × 1 cm (wide × length) with four different compositions. From the obtained data during the tensile test, the stress-strain curve was plotted, and finally, the slope of the stress-strain diagram was calculated based on the Hooks law to obtain the elastic modulus and the maximum point of the curve.

Morphological investigation of NCD

To evaluate the morphology, pore size, porosity, and geometry of the NCD, the scanning electron microscope (SEM) tools were used. To increase the electrical conductivity and to increase the sharpness and clearance of the images, the specimens were coated a skinny gold layer and then their surface morphology was investigated and image using XL30 model made by the Philips Company at the Amirkabir University of Technology, Central laboratory by South Korea SUORIN Company.

Phase investigation of NCD

The NCD and its final composition were characterized using XRD tools (X' Pert HighScore software) to provides comprehensive information on the crystallinity of all porous samples. The Scherrer equation is usually used to determine the average dimensions of crystals in XRD analysis. In this study, this analysis was also used to determine the phases present in NCD samples.

Biodegradation Test of NCD

The biodegradability of the wound dressing was investigated by monitoring the weight loss over 1, 3, 7,14, and 21 days incubated in phosphate buffer saline (PBS, pH 7.4) at room temperature. To calculate the sample degradation rate, NCD pieces with a dimension of 1 × 1 cm was prepared and selected from the final product. The porous NCD samples were stored in a CO_2 incubator at 37°C after being placed in a falcon tube containing 10 ml PBS. The initial weight of the NCD was written as W0 (wet weight), Wt (dry weight) and the NCD removed from the PBS after each time and then dried and weighed. The percentage of degradation was calculated using Eq. (1).

$$\text{Degradation rate of NCD}(\%) = \left(\frac{W_o - W_t}{W_o}\right) \times 100 \quad (1)$$

Biological responses of NCD

Since the wound is presented, and generally, all the products of tissue engineering are supposed to be related to the natural body's environment; therefore it is necessary to investigate some biological behavior such as the density behavior, ionic release and tissue changes after soaking in a biological solution related to the physiological conditions of the body. In the present study, ceramic reaction, antibacterial and toxicity test (MTT) have been applied to the porous specimen.

Toxicity Evaluation (MTT Assay)

MTT assay was carried out for cell viability and mitochondrial activity assessment. Living cells reduced the MTT substrate (3-[4,5-dimethylthiazol-2-yl]-2,5 diphenyltetrasodium bromide) to a dark-blue formazan in the presence of active mitochondria. Thus, an accurate measure of the mitochondrial

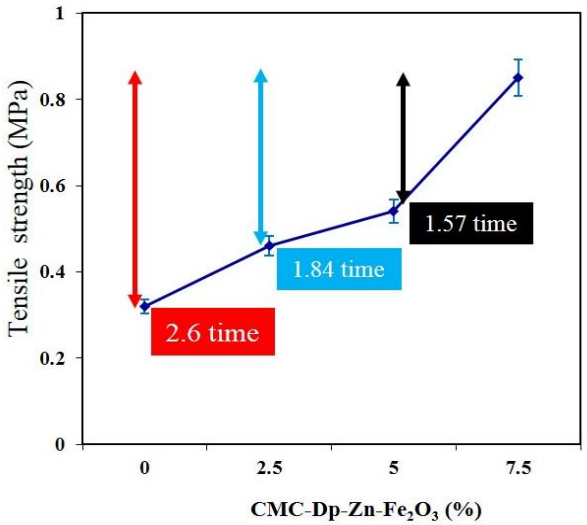

Fig. 3. Tensile strength of the NCD using SANTAM-STM50 containing 0 wt%, 2.5 wt%, 5 wt%, and 7.5 wt% Fe_2O_3.

Table 2. Mechanical properties of NCD function of Fe_2O_3 nanoparticles with various content

SAMPLE	Elastic Modulus (MPa)	Porosity (%)
CMC-Dp	32 ± 5	74 ± 4
CMC-DpZn	49 ± 5	79 ± 4
CMC-DpZn1	58 ± 4	81 ± 5
CMC-DpZn2	66 ± 5	84 ± 3

activity of cells in a culture medium was carried out [16, 26]. The MTT assay with fibroblast cells was used to evaluate the biocompatibility of the NCD samples. In this test, the cellular activity and cell viability are evaluated based on the activity of mitochondrial dehydrogenase enzymes in cells that are viable and active. The proper Cell line L929 (mouse tail fibroblast) prepared from New Technology Research Centre (CRLAB) was used for cytotoxicity and cell proliferation assay. After incubation, dimethyl sulfoxide (Sigma, USA) was added to dissolve the blue formazan crystals. Toxicity, as well as cell viability, were calculated by Eq. (2) and Eq. (3):

$$\text{Toxicity of NCD (\%)} = \left(1 - \frac{OD_{Sample}}{OD_{Control}}\right) \times 100 \qquad (2)$$

$$\text{Cell Viability of NCD}(\%) = 100 - \text{Toxicity \%} \qquad (3)$$

RESULTS AND DISCUSSION

In this work, the effect of the Dp incorporation on the tensile strength and elastic modulus of the NCD was studied to check the flexibility of the porous NCD that can control the wound infection and water absorption.

It is essential to know that one of the critical parameters in the discussion of wound dressing is the issue of tensile strength, as shown in Fig. 3. Also, Fig. 3 shows that by increasing 2.5 wt% MNPs amount, the tensile strength increase from 0.32 MPa to 0.46 MPa, and the sample containing the highest percentage of magnetic nanoparticles represents 0.85 MPa (2.6 times more than the sample without MNPs). Therefore, it can be claimed that the tensile strength enhanced with the addition of magnetic nanoparticles, although its porosity increased at the same time. The result of these changes is related to the amount of MNPs and microstructure of the additive represented in the SEM images and the XRD results. The mechanical value obtained from the experimental testing is shown in Table 2. Fig. 4 shows the elastic modulus changes for all the four NCD samples in which with the addition of MNPs the elastic modulus of the soft tissue increases from 32 MPa to 66 MPa, more than three times.

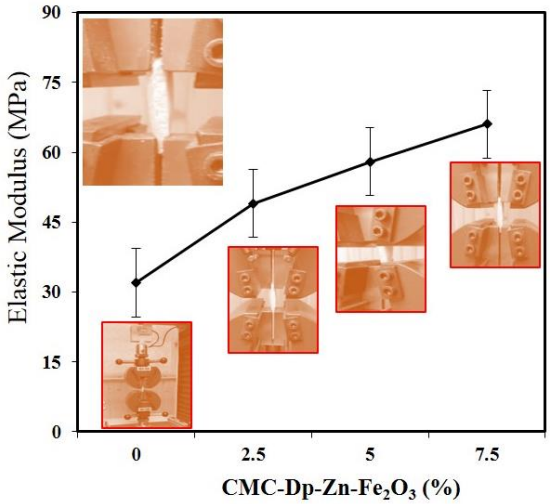

Fig. 4. Elastic modulus of NCD containing 0 wt%, 2.5 wt%, 5 wt%, and 7.5 wt% Fe_2O_3.

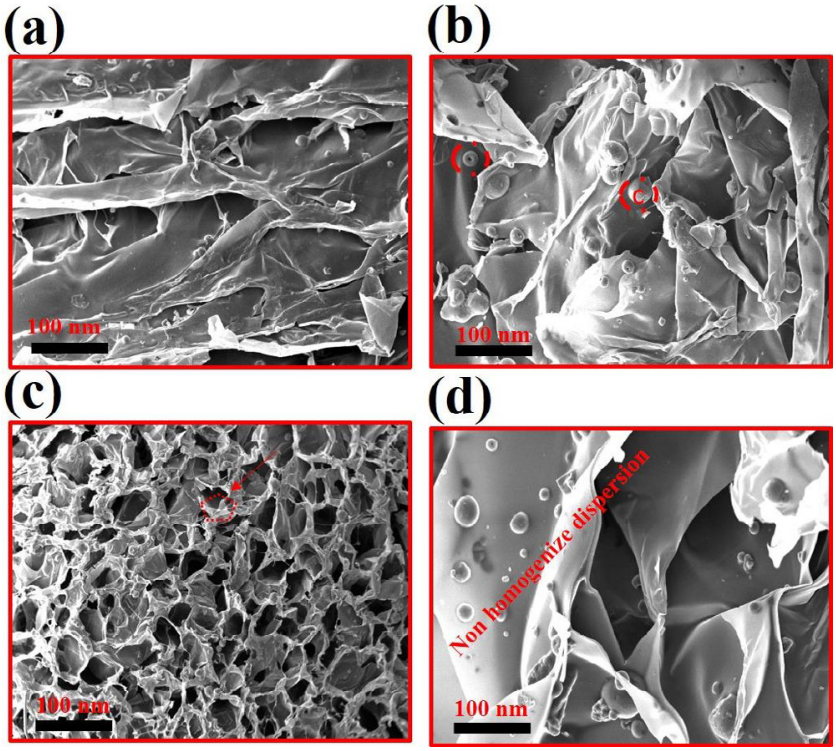

Fig. 5. SEM images of CMC/Dp-Zn-Fe_2O_3 concentrations of (a) 0 wt%, (b) 2.5 wt%, (c) 5 wt%, and (d) 7.5 wt% before immersion in PBS.

It is well known that a porous microstructure is important for the transport of oxygen and the promotion of drainage during the wound healing process. Therefore, the porosity of NCD samples with (0 wt%, 2.5 wt%, 5 wt% and 7.5 wt%) MNPs dispersed in the CMC-Dp was visualized using SEM images as shown in Fig. 5 (a-d).

Fig. 5 (a) shows that the particles are fused and chained together with the Dp nanoparticles regarding the similar surface to volume values and effect of their morphology. Fig. 5 (b) illustrates the sample with 2.5 wt% Fe_2O_3 nanoparticles with

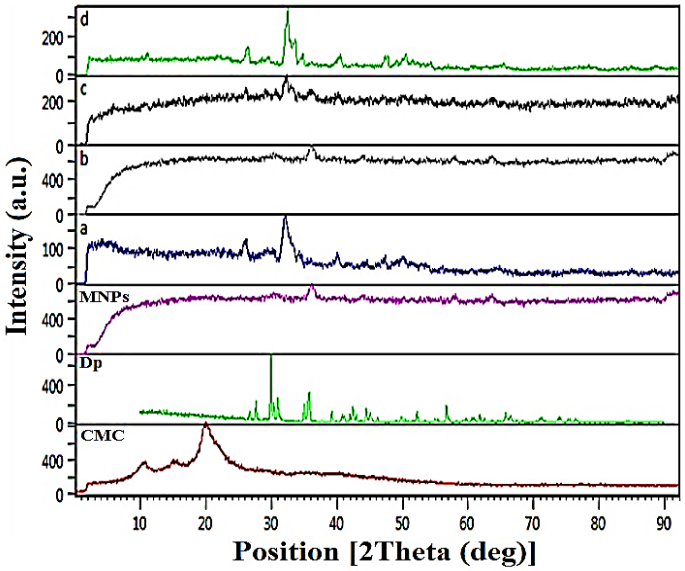

Fig. 6. XRD pattern of NCD with 0 wt%, 2.5 wt%, 5 wt%, and 7.5 wt% Fe_2O_3.

spherical particles resulting from the presence of bioceramic. Fig. 5 (c) shows the pores are homogeneous and interconnected pores with grid mode with 100-150 nm. The obtained results show that increasing magnetic material can increase the porosity and roughness of the NCD. However, this increase is not large enough to affect the physical properties of the NCD samples. Furthermore, according to Fig. 5(d), by increasing the magnetite content up to 7.5 wt%, the heterogeneous dispersion of the microparticles is well observable. The XRD pattern of all samples with different weight percentages of magnetic nanoparticles has been depicted in Fig. 6. Fig. 6 (a-d) shows the XRD spectrum of NCD with (a) 0 wt %, (b) 2.5wt %, (c) 5 wt% and (d) 7.5 wt% Fe_2O_3 nanoparticles. According to previous studies [13, 16, 59], the pure CMC has a weak peak at 10, which decreases with increasing bioceramic diopside. The obtained peak at position 20 degrees is the peak index of the nanocrystalline structure of the CMC polymer. Following the NCD crystallinity changes, the major peaks of the pure Dp nanocrystalline powder as well as the CMC polymer, occurred, which clearly indicates the presence of a proper bond between the polymer matrix and the ceramic powder.

The biodegradability results of the NCD sample are shown in Fig. 7. Fig. 7 shows that the NCD sample can absorb heavy elements from the PBS solution and leads to gain additional weight. In the sample with the lowest amount of MNPs, the heavy-ion absorption from the solution is lower despite great weight loss. On the other hand, the porosity value of NCD is also important in terms of weight loss and weight gain. It can be concluded that as the porosity decrease, then the weight loss of the NCD might decrease too. After careful visual observation of the sample the biological test shows that the sample, with a higher porosity value might have higher heavy ions release from their surface. Therefore, the sample's weight might be decreased or remain constant, which can be useful in the wound healing treatment process regarding the biofilm under the wound. The obtained results indicate that as the percentage of MNPs increases, water absorption and subsequent degradation rate increase. These findings can be attributed to the possible chemical bond between the nanoparticles and the CMC and the presence of iron ion groups in the composite microstructure that support the formation of physical, hydrogen bonds and ion interactions [60-68].

The cytotoxicity evaluation, known as the first test to evaluate the biocompatibility of soft tissue in the biomaterial domain, was performed to determine the fibroblast cell viability on NCD using the MTT assay. Therefore, as shown in Fig. 8, the cell viability on the surface of the porous wound dress was checked after 1, 3, 5 and 7 days of cell culture. Depending on the shape and size of the cell, one can say that cell growth and proliferation over time increased. On the third and fifth days of

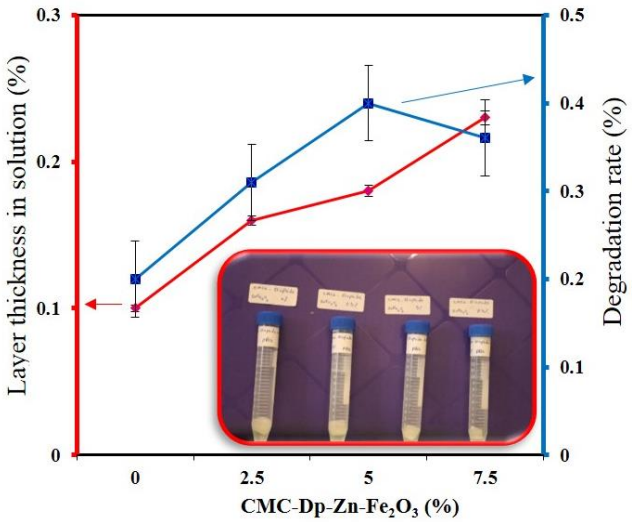

Fig. 7. Degradation rate and layer thickness of CMC/Dp with different percentages of Fe_2O_3 nanoparticles.

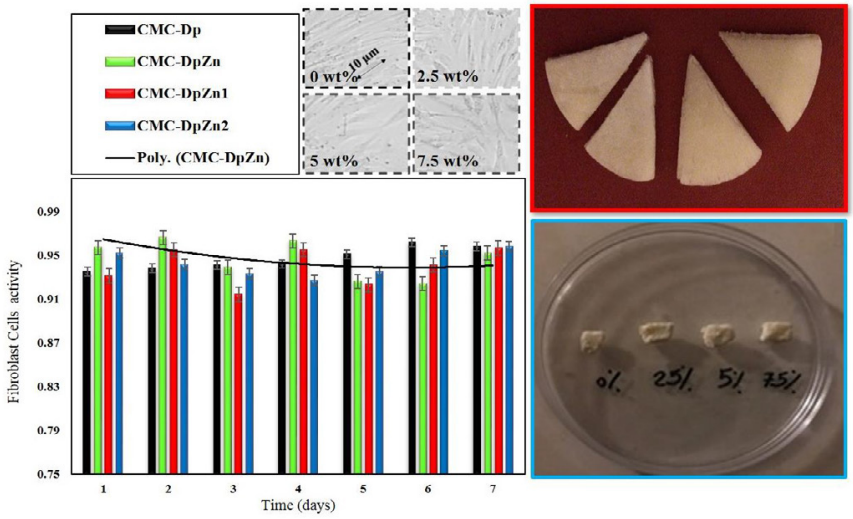

Fig. 8. Fibroblast Cells activity on NCD with 0 wt%, 2.5 wt%, 5 wt% and 7.5 wt% of Fe_2O_3.

cell culture, there was a significant difference in the number of cells in samples. It can be concluded that by the addition of MNPs content, the growth and viability of fibroblast cells increased in CMC-Dp, which is consistent with the results of previous studies [9, 11, 15, 33, 37, 38-40]. The cell culture observation illustrated that the cell viability on the surface of the sample containing 5 wt% and 7.5 wt% with higher porosity value increase due to the presence of a high percentage of magnetic nanoparticles compared to other samples. The porous structure may create a suitable substrate for cell interaction and proteins to attract each other. In fact, the results of this test show excellent biocompatibility of all four samples due to their higher adsorption rate compared to the control sample [70-75].

CONCLUSION

The NCD with MNPs were synthesized through FD technique. In fact, due to the hydrophilic properties, consequently the poor mechanical properties of CMC in the presence of water and biological environments and the inadequacy of hardness, it may need some reinforcement to overcome the limitations of polymer with

bioceramic composition as well as enhance the antibacterial properties of the wound site. The properties of the wound dress were investigated including morphology, mechanical properties, antibacterial property, and biocompatibility response. The obtained results were characterized using XRD and SEM analysis and compared with the control sample. The SEM images showed that the scaffolds prepared by this method had interconnected pores. Then, it was concluded as the magnetic and ceramic phases increased, both tensile and porosity values increase which related to the NCD microstructure. The composite was found to have a favorable pore size of about 50 µm with 70-90% porosity. The size of pores in composite scaffolds increased and the sample containing 5 wt% Fe_2O_3 magnetic nanoparticles had the optimum microstructure in terms of the number of cavities and uniformity of the created interconnected porosity. The mechanical and biological characteristics of fabricated NCD were influenced by the addition of MNPs and Dp content that substantially improved cell attachment on the scaffold surfaces and increases the elastic modulus. Therefore, based on the studies and evaluations, it can be concluded that the addition of Dp increases the tensile strength and the addition of magnetic nanoparticles has a significant effect on the antibacterial property of the wound dress. It can be concluded that CMC nanocomposite containing 5 wt% of Fe_2O_3 magnetic nanoparticles prepared by freeze-drying technique has a potential application for wound healing approaches.

CONFLICT OF INTEREST

The authors declare that they have no conflict of interest.

REFERENCES

1. Bagher Z, Ehterami A, Safdel MH, Khastar H, Semiari H, Asefnejad A, et al. Wound healing with alginate/chitosan hydrogel containing hesperidin in rat model. Journal of Drug Delivery Science and Technology. 2020;55:101379.
2. Ying H, Zhou J, Wang M, Su D, Ma Q, Lv G, et al. In situ formed collagen-hyaluronic acid hydrogel as biomimetic dressing for promoting spontaneous wound healing. Materials Science and Engineering: C. 2019;101:487-98.
3. Asefnejad A, Khorasani, Behnamghader, Bonakdar. Manufacturing of biodegradable polyurethane scaffolds based on polycaprolactone using a phase separation method: physical properties and in vitro assay. International Journal of Nanomedicine. 2011:2375.
4. Biazar, E., Rezayat, S. M., Montazeri, N., Pourshamsian, K., Zeinali, R., Asefnejad, A., ... & Ziaei, M. (2010). The effect of acetaminophen nanoparticles on liver toxicity in a rat model. *International journal of nanomedicine*, *5*, 197.
5. Seyfi J, Panahi-Sarmad M, OraeiGhodousi A, Goodarzi V, Khonakdar HA, Asefnejad A, et al. Antibacterial superhydrophobic polyvinyl chloride surfaces via the improved phase separation process using silver phosphate nanoparticles. Colloids and Surfaces B: Biointerfaces. 2019;183:110438.
6. Jalili, M., Mozaffari, A., Gashti, M., & Parsania, M. (2019). Electrospinning Nanofibers Gelatin scaffolds: Nanoanalysis of properties and optimizing the process for tissue engineering functional. parameters, 4(16), 8.
7. Shojaie S, Rostamian M, Samadi A, Alvani MAS, Khonakdar HA, Goodarzi V, et al. Electrospun electroactive nanofibers of gelatin-oligoaniline/Poly (vinyl alcohol) templates for architecting of cardiac tissue with on-demand drug release. Polymers for Advanced Technologies. 2019;30(6):1473-83.
8. Kamyab Moghadas, B., & Azadi, M. (2019). Fabrication of Nanocomposite Foam by Supercritical CO2 Technique for Application in Tissue Engineering. *Journal of Tissues and Materials*, *2*(1), 23-32.
9. Moghadas BK, Akbarzadeh A, Azadi M, Aghili A, Rad AS, Hallajian S. The morphological properties and biocompatibility studies of synthesized nanocomposite foam from modified polyethersulfone/graphene oxide using supercritical CO2. Journal of Macromolecular Science, Part A. 2020;57(6):451-60.
10. Haghayegh M, Zabihi F, Eikani MH, Kamya Moghadas B, Vaziri Yazdi SA. Supercritical Fluid Extraction of Flavonoids and Terpenoids from Herbal compounds: Experiments and Mathematical modeling. Journal of Essential Oil Bearing Plants. 2015;18(5):1253-65.
11. Abd-Khorsand S, Saber-Samandari S, Saber-Samandari S. Development of nanocomposite scaffolds based on TiO 2 doped in grafted chitosan/hydroxyapatite by freeze drying method and evaluation of biocompatibility. International Journal of Biological Macromolecules. 2017;101:51-8.
12. Kordjamshidi A, Saber-Samandari S, Ghadiri Nejad M, Khandan A. Preparation of novel porous calcium silicate scaffold loaded by celecoxib drug using freeze drying technique: Fabrication, characterization and simulation. Ceramics International. 2019;45(11):14126-35.
13. Saber-Samandari S, Saber-Samandari S, Kiyazar S, Aghazadeh J, Sadeghi A. In vitro evaluation for apatite-forming ability of cellulose-based nanocomposite scaffolds for bone tissue engineering. International Journal of Biological Macromolecules. 2016;86:434-42.
14. Saber-Samandari S, Saber-Samandari S, Ghonjizade-Samani F, Aghazadeh J, Sadeghi A. Bioactivity evaluation of novel nanocomposite scaffolds for bone tissue engineering: The impact of hydroxyapatite. Ceramics International. 2016;42(9):11055-62.
15. Saber-Samandari S, Saber-Samandari S. Biocompatible nanocomposite scaffolds based on copolymer-grafted chitosan for bone tissue engineering with drug delivery capability. Materials Science and Engineering: C. 2017;75:721-32.
16. Beladi F, Saber-Samandari S, Saber-Samandari S. Cellular compatibility of nanocomposite scaffolds based on hydroxyapatite entrapped in cellulose network for bone repair. Materials Science and Engineering: C. 2017;75:385-92.
17. Saber-Samandari S, Gross KA. Micromechanical properties of single crystal hydroxyapatite by nanoindentation. Acta Biomaterialia. 2009;5(6):2206-12.

18. Farazin, A., Aghadavoudi, F., Motififard, M., Saber-Samandari, S., & Khandan, A. (2020). Nanostructure, molecular dynamics simulation and mechanical performance of PCL membranes reinforced with antibacterial nanoparticles. *Journal of Applied and Computational Mechanics*.
19.Farazin, A., Aghdam, H. A., Motififard, M., Aghadavoudi, F., Kordjamshidi, A., Saber-Samandari, S., & Khandan, A. (2019). A polycaprolactone bio-nanocomposite bone substitute fabricated for femoral fracture approaches: Molecular dynamic and micro-mechanical Investigation. *J Nanoanaly*.
20. Mogoşanu GD, Grumezescu AM. Natural and synthetic polymers for wounds and burns dressing. International Journal of Pharmaceutics. 2014;463(2):127-36.
21. Wang Y, Li P, Xiang P, Lu J, Yuan J, Shen J. Electrospun polyurethane/keratin/AgNP biocomposite mats for biocompatible and antibacterial wound dressings. Journal of Materials Chemistry B. 2016;4(4):635-48.
22. Ahmed S, Ikram S. Chitosan Based Scaffolds and Their Applications in Wound Healing. Achievements in the Life Sciences. 2016;10(1):27-37.
23. Campos M, Cordi L, Durán N, Mei L. Antibacterial Activity of Chitosan Solutions for Wound Dressing. Macromolecular Symposia. 2006;245-246(1):515-8.
24. Keong LC, Halim AS. In Vitro Models in Biocompatibility Assessment for Biomedical-Grade Chitosan Derivatives in Wound Management. International Journal of Molecular Sciences. 2009;10(3):1300-13.
25. Sanad RA-B, Abdel-Bar HM. Chitosan–hyaluronic acid composite sponge scaffold enriched with Andrographolide-loaded lipid nanoparticles for enhanced wound healing. Carbohydrate Polymers. 2017;173:441-50.
26. Edwards N, Feliers D, Zhao Q, Stone R, Christy R, Cheng X. An electrochemically deposited collagen wound matrix combined with adipose-derived stem cells improves cutaneous wound healing in a mouse model of type 2 diabetes. Journal of Biomaterials Applications. 2018;33(4):553-65.
27. Rafienia M, Salami M, Kaveian F, Saber-Samandari S, Khandan A, Naeimi M. Electrospun Polycaprolactone/lignin-based Nanocomposite as a Novel Tissue Scaffold for Biomedical Applications. Journal of Medical Signals & Sensors. 2017;7(4):228.
28.Maghsoudlou, M. A., Nassireslami, E., Saber-Samandari, S., & Khandan, A. (2020). Bone Regeneration Using Bio-Nanocomposite Tissue Reinforced with Bioactive Nanoparticles for Femoral Defect Applications in Medicine. *Avicenna Journal of Medical Biotechnology*, *12*(2).
29.Khandan, A., Jazayeri, H., Fahmy, M. D., & Razavi, M. (2017). Hydrogels: Types, structure, properties, and applications. *Biomat Tiss Eng*, *4*(27), 143-69.
30. Razavi M, Khandan A. Safety, regulatory issues, long-term biotoxicity, and the processing environment. Nanobiomaterials Science, Development and Evaluation: Elsevier; 2017. p. 261-79.
31. Sahmani S, Khandan A, Saber-Samandari S, Mohammadi Aghdam M. Effect of magnetite nanoparticles on the biological and mechanical properties of hydroxyapatite porous scaffolds coated with ibuprofen drug. Materials Science and Engineering: C. 2020;111:110835.
32.Lieberman, J. R., Daluiski, A., & Einhorn, T. A. (2002). The role of growth factors in the repair of bone: biology and clinical applications. JBJS, 84(6), 1032-1044.
33. Sahmani S, Saber-Samandari S, Khandan A, Aghdam MM. Influence of MgO nanoparticles on the mechanical properties of coated hydroxyapatite nanocomposite scaffolds produced via space holder technique: Fabrication, characterization and simulation. Journal of the Mechanical Behavior of Biomedical Materials. 2019;95:76-88.
34. Sahmani S, Shahali M, Ghadiri Nejad M, Khandan A, Aghdam MM, Saber-Samandari S. Effect of copper oxide nanoparticles on electrical conductivity and cell viability of calcium phosphate scaffolds with improved mechanical strength for bone tissue engineering. The European Physical Journal Plus. 2019;134(1).
35. Sahmani S, Saber-Samandari S, Shahali M, Joneidi Yekta H, Aghadavoudi F, Montazeran AH, et al. Mechanical and biological performance of axially loaded novel bio-nanocomposite sandwich plate-type implant coated by biological polymer thin film. Journal of the Mechanical Behavior of Biomedical Materials. 2018;88:238-50.
36. Saber-Samandari S, Gross KA. Amorphous calcium phosphate offers improved crack resistance: A design feature from nature? Acta Biomaterialia. 2011;7(12):4235-41.
37. Saber-Samandari S, Gross KA. Effect of angled indentation on mechanical properties. Journal of the European Ceramic Society. 2009;29(12):2461-7.
38. Sahmani S, Khandan A, Saber-Samandari S, Aghdam MM. Vibrations of beam-type implants made of 3D printed bredigite-magnetite bio-nanocomposite scaffolds under axial compression: Application, communication and simulation. Ceramics International. 2018;44(10):11282-91.
39. Sahmani S, Khandan A, Saber-Samandari S, Aghdam MM. Nonlinear bending and instability analysis of bioceramics composed with magnetite nanoparticles: Fabrication, characterization, and simulation. Ceramics International. 2018;44(8):9540-9.
40. Sahmani S, Shahali M, Khandan A, Saber-Samandari S, Aghdam MM. Analytical and experimental analyses for mechanical and biological characteristics of novel nanoclay bio-nanocomposite scaffolds fabricated via space holder technique. Applied Clay Science. 2018;165:112-23.
41. Abdellahi M, Najafinezhad A, Ghayour H, Saber-Samandari S, Khandan A. Preparing diopside nanoparticle scaffolds via space holder method: Simulation of the compressive strength and porosity. Journal of the Mechanical Behavior of Biomedical Materials. 2017;72:171-81.
42. Kazemi A, Abdellahi M, Khajeh-Sharafabadi A, Khandan A, Ozada N. Study of in vitro bioactivity and mechanical properties of diopside nano-bioceramic synthesized by a facile method using eggshell as raw material. Materials Science and Engineering: C. 2017;71:604-10.
43. Najafinezhad A, Abdellahi M, Ghayour H, Soheily A, Chami A, Khandan A. A comparative study on the synthesis mechanism, bioactivity and mechanical properties of three silicate bioceramics. Materials Science and Engineering: C. 2017;72:259-67.
44. Khandan A, Ozada N, Saber-Samandari S, Ghadiri Nejad M. On the mechanical and biological properties of bredigite-magnetite (Ca7MgSi4O16-Fe3O4) nanocomposite scaffolds. Ceramics International. 2018;44(3):3141-8.
45.Montazeran, A. H., Saber Samandari, S., & Khandan, A. (2018). Artificial intelligence investigation of three silicates bioceramics-magnetite bio-nanocomposite: Hyperthermia and biomedical applications. *Nanomedicine Journal*, *5*(3), 163-171.

46.Joneidi Yekta, H., Shahali, M., Khorshidi, S., Rezaei, S., Montazeran, A. H., Samandari, S. S., ... & Khandan, A. (2018). Mathematically and experimentally defined porous bone scaffold produced for bone substitute application. *Nanomedicine Journal*, *5*(4), 227-234.
47. Sahmani S, Saber-Samandari S, Aghdam MM, Khandan A. Nonlinear Resonance Response of Porous Beam-Type Implants Corresponding to Various Morphology Shapes for Bone Tissue Engineering Applications. Journal of Materials Engineering and Performance. 2018;27(10):5370-83.
48. Naga SM, El-Maghraby HF, Mahmoud EM, Killinger A, Gadow R. Hydroxyapatite/Diopside Porous Scaffolds: Preparation and In Vitro Study. Interceram - International Ceramic Review. 2019;68(4):22-9.
49. Ghayour H, Abdellahi M, Ozada N, Jabbrzare S, Khandan A. Hyperthermia application of zinc doped nickel ferrite nanoparticles. Journal of Physics and Chemistry of Solids. 2017;111:464-72.
50. Ghayour H, Abdellahi M, Nejad MG, Khandan A, Saber-Samandari S. Study of the effect of the Zn2 + content on the anisotropy and specific absorption rate of the cobalt ferrite: the application of Co1 − x Zn x Fe2O4 ferrite for magnetic hyperthermia. Journal of the Australian Ceramic Society. 2017;54(2):223-30.
51. Webster TJ, Ergun C, Doremus RH, Bizios R. Hydroxylapatite with substituted magnesium, zinc, cadmium, and yttrium. II. Mechanisms of osteoblast adhesion. Journal of Biomedical Materials Research. 2001;59(2):312-7.
52.Monshi, M., Esmaeili, S., Kolooshani, A., Moghadas, B. K., Saber-Samandari, S., & Khandan, A. (2020). A novel three-dimensional printing of electroconductive scaffolds for bone cancer therapy application. *Nanomedicine Journal*, *7*(2), 138-148.
53.Esmaeili, S., Shahali, M., Kordjamshidi, A., Torkpoor, Z., Namdari, F., Samandari, S. S., ... & Khandan, A. (2019). An artificial blood vessel fabricated by 3D printing for pharmaceutical application. *Nanomedicine Journal*, *6*(3), 183-194.
54.Hashemi, S., Esmaeili, S., Ghadirinejad, M., Saber-Samandari, S., Sheikhbahaei, E., Kordjamshidi, A., Khandan, A. (2020). Micro-Finite Element Model to Investigate the Mechanical Stimuli in Scaffolds Fabricated via Space Holder Technique for Cancellous Bone. *ADMT Journal*, 13(1), 51-58.
55.Bagheri, S., Hashemian, M., Khosravi, M., & Khandan, A. (2020). An experimental investigation of novel hybrid epoxy/glass fibers nanocomposite reinforced with nanoclay with enhanced properties for low velocity impact test. *Journal of Nanostructures*, *10*(1), 92-106.
56. Esmaeili S, Akbari Aghdam H, Motififard M, Saber-Samandari S, Montazeran AH, Bigonah M, et al. A porous polymeric–hydroxyapatite scaffold used for femur fractures treatment: fabrication, analysis, and simulation. European Journal of Orthopaedic Surgery & Traumatology. 2019;30(1):123-31.
57. Akbari Aghdam H, Sanatizadeh E, Motififard M, Aghadavoudi F, Saber-Samandari S, Esmaeili S, et al. Effect of calcium silicate nanoparticle on surface feature of calcium phosphates hybrid bio-nanocomposite using for bone substitute application. Powder Technology. 2020;361:917-29.
58.Tahririan, M. A., Motififard, M., Omidian, A., Aghdam, H. A., & Esmaeali, A. (2017). Relationship between bone mineral density and serum vitamin D with low energy hip and distal radius fractures: A case-control study. *Archives of Bone and Joint Surgery*, *5*(1), 22.
59. Akbari Aghdam H, Sheikhbahaei E, Hajihashemi H, Kazemi D, Andalib A. The impacts of internal versus external fixation for tibial fractures with simultaneous acute compartment syndrome. European Journal of Orthopaedic Surgery & Traumatology. 2018;29(1):183-7.
60. Moghimi Monfared R, Ayatollahi MR, Barbaz Isfahani R. Synergistic effects of hybrid MWCNT/nanosilica on the tensile and tribological properties of woven carbon fabric epoxy composites. Theoretical and Applied Fracture Mechanics. 2018;96:272-84.
61. Ayatollahi MR, Barbaz Isfahani R, Moghimi Monfared R. Effects of multi-walled carbon nanotube and nanosilica on tensile properties of woven carbon fabric-reinforced epoxy composites fabricated using VARIM. Journal of Composite Materials. 2017;51(30):4177-88.
62. Maghsoudlou MA, Barbaz Isfahani R, Saber-Samandari S, Sadighi M. Effect of interphase, curvature and agglomeration of SWCNTs on mechanical properties of polymer-based nanocomposites: Experimental and numerical investigations. Composites Part B: Engineering. 2019;175:107119.
63. Ayatollahi MR, Moghimi Monfared R, Barbaz Isfahani R. Experimental investigation on tribological properties of carbon fabric composites: effects of carbon nanotubes and nano-silica. Proceedings of the Institution of Mechanical Engineers, Part L: Journal of Materials: Design and Applications. 2017;233(5):874-84.
64. Kamarian S, Bodaghi M, Isfahani RB, Shakeri M, Yas MH. Influence of carbon nanotubes on thermal expansion coefficient and thermal buckling of polymer composite plates: experimental and numerical investigations. Mechanics Based Design of Structures and Machines. 2019;49(2):217-32.
65.Barbaz-I, R. (2014). *Experimental determining of the elastic modulus and strength of composites reinforced with two nanoparticles* (Doctoral dissertation, MSc Thesis, School of Mechanical Engineering Iran University of Science and Technology, Tehran, Iran).
66. Moeini M, Barbaz Isfahani R, Saber-Samandari S, Aghdam MM. Molecular dynamics simulations of the effect of temperature and strain rate on mechanical properties of graphene–epoxy nanocomposites. Molecular Simulation. 2020;46(6):476-86.
67.Mirzaalian, M., Aghadavoudi, F., & Moradi-Dastjerdi, R. (2019). Bending Behavior of Sandwich Plates with Aggregated CNT-Reinforced Face Sheets. *Journal of Solid Mechanics*, *11*(1), 26-38.
68. Moradi-Dastjerdi R, Aghadavoudi F. Static analysis of functionally graded nanocomposite sandwich plates reinforced by defected CNT. Composite Structures. 2018;200:839-48.
69. Razmjooee K, Saber-Samandari S, Keshvari H, Ahmadi S. Improving anti thrombogenicity of nanofibrous polycaprolactone through surface modification. Journal of Biomaterials Applications. 2019;34(3):408-18.
70. Zamani D, Razmjooee K, Moztarzadeh F, Bizari D. Synthesis and Characterization of Alginate Scaffolds Containing Bioactive Glass for Bone Tissue Engineering Applications. 2017 24th National and 2nd International Iranian Conference on Biomedical Engineering (ICBME); 2017/11: IEEE; 2017.
71.Saber-Samandari, S., Yekta, H., & Saber-Samandari, S. (2015). Effect of iron substitution in hydroxyapatite matrix on swelling properties of composite bead. *JOM*, *9*(1), 19-25.
72. Saber-Samandari S, Yekta H, Ahmadi S, Alamara K. The

role of titanium dioxide on the morphology, microstructure, and bioactivity of grafted cellulose/hydroxyapatite nanocomposites for a potential application in bone repair. International Journal of Biological Macromolecules. 2018;106:481-8.
73. Moradi-Dastjerdi R, Malek-Mohammadi H, Momeni-Khabisi H. Free vibration analysis of nanocomposite sandwich plates reinforced with CNT aggregates. ZAMM - Journal of Applied Mathematics and Mechanics / Zeitschrift für Angewandte Mathematik und Mechanik. 2017.
74. Moradi-Dastjerdi R, Payganeh G, Tajdari M. Thermoelastic analysis of functionally graded cylinders reinforced by wavy CNT using a mesh-free method. Polymer Composites. 2016;39(7):2190-201.
75. Moradi-Dastjerdi R, Payganeh G, Tajdari M. Resonance in functionally graded nanocomposite cylinders reinforced by wavy carbon nanotube. Polymer Composites. 2016;38:E542-E52.